Journal of the Faculty of Environmental Science and Technology, Okayama University
Vol.3, No.1, pp.11-24, January 1998

A numerical analysis of slow oscillations in dynamics of coupled systems

Masaji Watanabe *

(Received October 31 , 1997)

Abstract

We study a system that models a problem in which an oscillatory unit is coupled to a passive medium. We analyze the case in which an RCL circuit is coupled to an RC circuit. Some numerical results indicate when slow oscillations occur in coupled systems.

KEYWORDS: coupled circuits, Van der Pol's equation, slow oscillations.

1. Introduction

We study a system that can generate an oscillatory dynamics with a large period out of a fast oscillator. Suppose that the state of some oscillatory unit is governed by the following n-dimensional system when the unit is isolated from a surrounding medium.

$$\frac{dx_1}{dt} = f(x_1). \tag{1}$$

Suppose also that the unit is coupled to a passive medium, and that the states of the unit and the medium are governed by the following system.

$$\begin{aligned} \frac{dx_1}{dt} &= f(x_1) + \delta P(x_0 - x_1), \\ \frac{dx_0}{dt} &= \epsilon \delta P(x_1 - x_0). \end{aligned} \tag{2}$$

Here x_0 represents the state of the medium and x_1 represents the state of the unit. ϵ is defined by $\epsilon = V_1/V_0$, where V_1 is the volume of the unit and V_0 is the volume of the medium. P is an $n \times n$ constant matrix of permeability coefficients, and δ is the parameter which measures the coupling strength. A biological problem for which (2) is a model is found in [2]. We assume that the (1) has an oribitally asymptotically stable periodic solution $x_1 = \eta(t)$ of least period $T > 0$. Periodic solutions of (2) in case the eigenvalues of P all have positive real parts are studied in [4] and [5]. Here we study the case P is singular. Specifically, we assume that

$$P = \begin{bmatrix} 0 & 0 \\ 0 & 1 \end{bmatrix},$$

and that (1) is the following planar system.

$$\begin{aligned} \kappa \frac{dv}{dt} &= g(v, w), \\ \frac{dw}{dt} &= h(v, w). \end{aligned} \tag{3}$$

*Department of Environmental and Mathematical Sciences, Faculty of Environmental Science and Technology, Okayama University, Okayama 700, Japan. Supported by a Grant-in-Aid for Scientific Research (C) from the Ministry of Education, Science, Sports, and Culture.

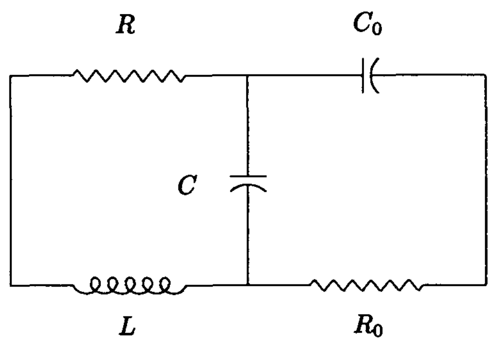

Figure 1: Coupled electrical circuits. An RCL circuit has a resistor R, an inductor L, and a capacitor C. An RC circuit has a resistor R_0 and a capacitor C_0. The RCL circuit is coupled to the RC circuit.

Here we assume that $\kappa > 0$. Under the assumptions made in Section 2, (3) has an orbitally asymptotically periodic solution for all sufficiently small $\kappa > 0$. Now (2) becomes

$$\begin{aligned} \kappa \frac{dv}{dt} &= g(v,w), \\ \frac{dw}{dt} &= h(v,w) + \delta p(w,x), \\ \frac{dx}{dt} &= -\epsilon \delta p(w,x), \end{aligned} \tag{4}$$

where $p(w,x) = (x - w)$. Coupled electrical circuits give rise to an example of such a system. Suppose that an RCL circuit is coupled to an RC circuit (cf. Figure 1), and that the uncoupled RCL circuit is modeled by the following system.

$$\begin{aligned} L\frac{di_L}{d\tau} &= v_C - F(i_L), \\ C\frac{dv_C}{d\tau} &= -i_L. \end{aligned} \tag{5}$$

Here i_L is the current through the inductor L and v_C is the voltage drop at the capacitor C. The characteristic of the resistor R is the graph of $v_R = F(i_R)$ in the (i_R, v_R) plane. Here i_R is the current through the resistor R and v_R is the voltage drop at the resistor. We assume that $F(x) = x^3 - x$. L is the inductance of the inductor L and C is the capacitance of the capacitor C. For $L = 1$ and for $C = 1$, (5) is Van der Pol's equation. The dynamics of the coupled circuits is governed by the following system.

$$\begin{aligned} L\frac{di_L}{d\tau} &= v_C - f(i_L), \\ C\frac{dv_C}{d\tau} &= -i_L + \tfrac{1}{R_0}(v_{C_0} - v_C), \\ C_0\frac{dv_{C_0}}{d\tau} &= -\tfrac{1}{R_0}(v_{C_0} - v_C). \end{aligned} \tag{6}$$

Here v_{C_0} is the voltage drop at the capacitor C_0, and C_0 is the capacitance of the capacitor. The characteristic of the resistor R_0 is $v_{R_0} = R_0 i_{R_0}$ in the (i_{R_0}, v_{R_0}) plane. Here i_{R_0} is the current through the resistor R_0 and v_{R_0} is the voltage drop at the resistor.

The substitutions $\tau = Ct$, $v = -i_L$, $w = v_C$, and $x = v_{C_0}$ in (5) and (6) lead to the following systems.

$$\begin{aligned} \kappa \frac{dv}{dt} &= -w - \left(v^3 - v\right), \\ \frac{dw}{dt} &= v. \end{aligned} \tag{7}$$

$$\begin{aligned} \kappa \frac{dv}{dt} &= -w - \left(v^3 - v\right), \\ \frac{dw}{dt} &= v + \delta\left(x - w\right), \\ \frac{dx}{dt} &= -\epsilon\delta\left(x - w\right). \end{aligned} \tag{8}$$

When the functions $g(v,w)$, $h(v,w)$, and $p(w,x)$ are defined by

$$\begin{aligned} g(v,w) &= -w - \left(v^3 - v\right), \\ h(v,w) &= v, \\ p(w,x) &= x - w, \end{aligned}$$

and when the parameters κ, δ, and ϵ are given by

$$\begin{aligned} \kappa &= \frac{L}{C}, \\ \delta &= \frac{1}{R_0}, \\ \epsilon &= \frac{C}{C_0}, \end{aligned}$$

we find that (7) and (8) are special cases of (3) and (4), respectively. In Sections 2 and 3, we show some numerical results concerning (8).

2. Systems in the Singular Limit

We assume that the v-nullcline of (3) is given by a smooth function $w = \alpha(v)$, and that

$$\alpha'(v) = \begin{cases} < 0, & v < v_\ell, \\ > 0, & v_\ell < v < v_r, \\ < 0, & v > v_r, \end{cases}$$

$$g_w(v, \alpha(v)) < 0 \text{ for all } v \in \mathbf{R},$$

$$g_{vv}(v_\ell, w_\ell) \neq 0, \quad w_\ell = \alpha(v_\ell),$$

$$g_{vv}(v_r, w_r) \neq 0, \quad w_r = \alpha(v_r).$$

We also assume that $h_v(v,w) > 0$ for all $(v,w) \in \mathbf{R}^2$, and that the w-nullcline of (3) is a smooth curve which intersects the v-nullcline exactly at one point (v_0, w_0) with $v_\ell < v_0 < v_r$. Note that (7) meets these requirements. Figure 2 shows the nullclines of (7). Under these assumptions, (3) has a periodic solution for sufficiently small $\kappa > 0$ [1]. Some examples of such periodic solutions are numerically generated, and shown in Figures 3 and 4.

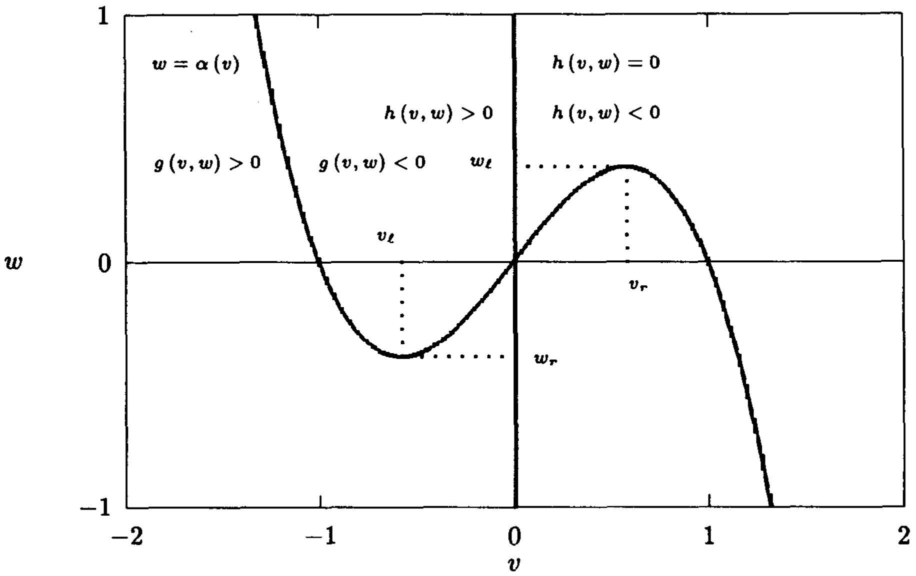

Figure 2: The nullclines of the planar system. The nullclines of (7) are shown.

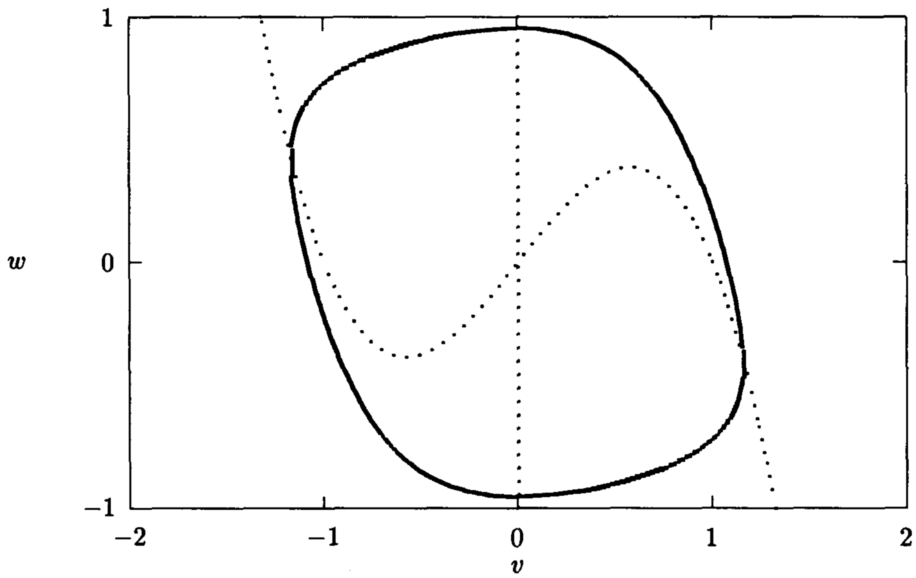

Figure 3: A closed orbit of the planar system. A periodic solution of (7) for $\kappa = 0.5$ is numerically generated, and its orbit is shown. The period T of the periodic solution is given approximately by $T \approx 4.969327$.

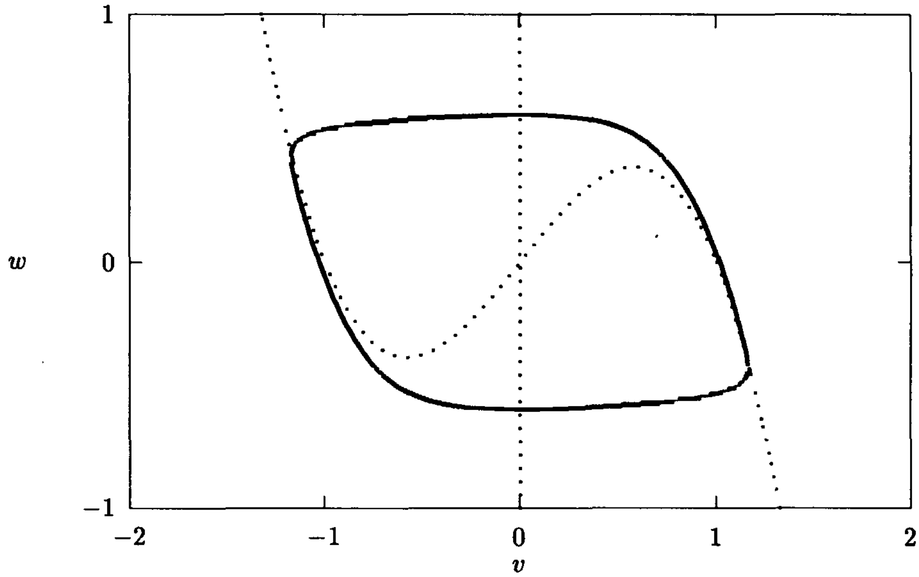

Figure 4: A closed orbit of the planar system. A periodic solution of (7) for $\kappa = 0.1$ is numerically generated, and its orbit is shown. The period T of the periodic solution is given approximately by $T \approx 2.878519$.

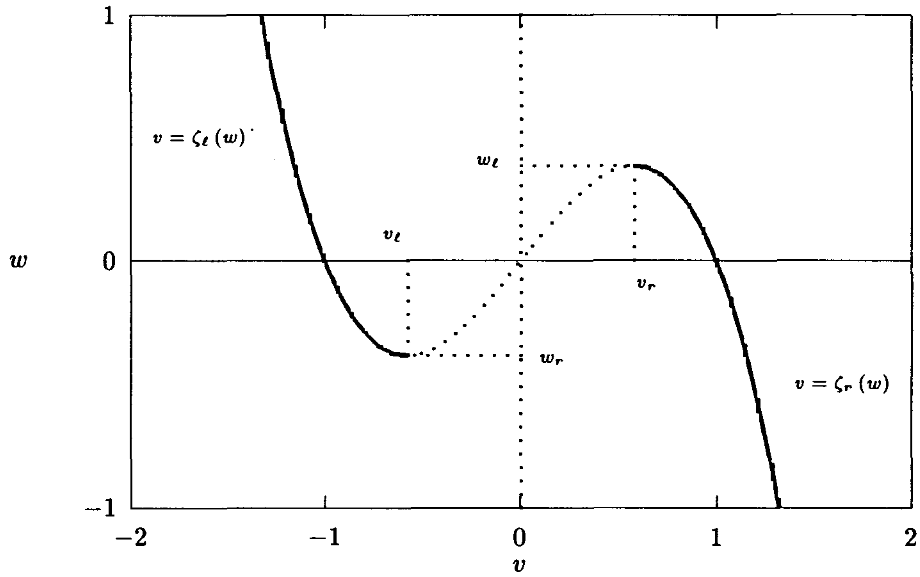

Figure 5: The inverse functions of $w = \alpha(v)$. $w = \alpha(v)$ is v-nullcline of (7). $v = \zeta_\ell(w)$ and $v = \zeta_r(w)$ are defined on the intervals (w_ℓ, ∞) and $(-\infty, v_r)$, respectively.

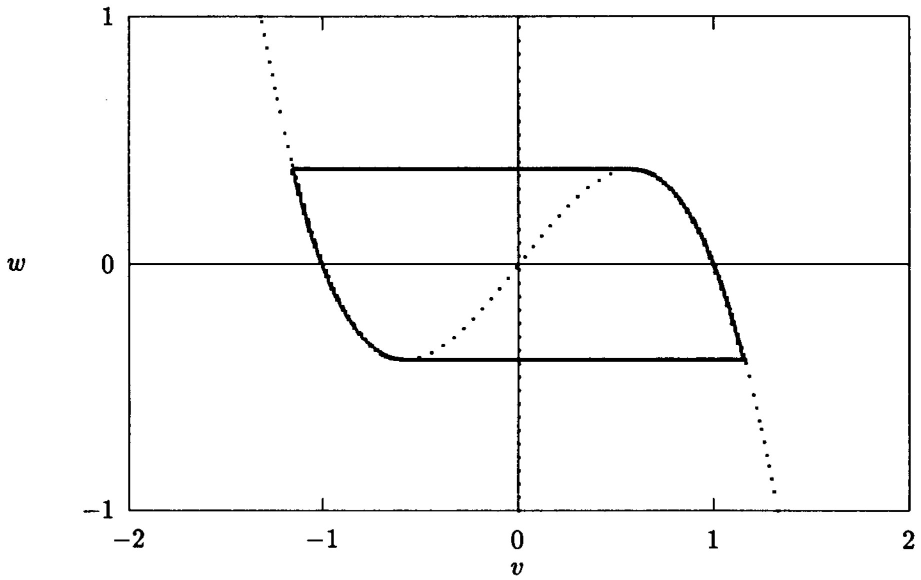

Figure 6: The discontinuous periodic solution. The orbit of the discontinuous periodic solution of (7) in the limit $\kappa \longrightarrow 0$ is shown.

We denote by $v = \zeta_\ell(w)$ the inverse function of $w = \alpha(v)$ defined on the interval (w_ℓ, ∞). and by $v = \zeta_r(w)$ the inverse function of $w = \alpha(v)$ defined on the interval $(-\infty, v_r)$ (cf. Figure 5). For sufficiently small $\kappa > 0$, the solutions of (3) are approximated by the solutions in the limit $\kappa \longrightarrow 0$. In the limit $\kappa \longrightarrow 0$, the solutions are restricted either to the curve $v = \zeta_\ell(w)$ or to the curve $v = \zeta_r(w)$. The solutions in the curves $v = \zeta_\ell(w)$ and $v = \zeta_r(w)$ are governed by the following equations (9) and (10), respectively.

$$\frac{dw}{dt} = h(\zeta_\ell(w), w), \tag{9}$$

$$\frac{dw}{dt} = h(\zeta_r(w), w). \tag{10}$$

In particular, the system has a discontinuous periodic solution (cf. Figure 6). The period T of this periodic solution is given by

$$T = \int_{w_r}^{w_\ell} \frac{dw}{h(\zeta_\ell(w), w)} + \int_{w_\ell}^{w_r} \frac{dw}{h(\zeta_r(w), w)}.$$

In the limit $\kappa \longrightarrow 0$, the solutions of (7) are restricted either to the region Ω_ℓ defined by

$$\Omega_\ell = \{(v, w, x) \,|v = \zeta_\ell(w), w \geq w_\ell\}$$

or to the region Ω_r defined by

$$\Omega_r = \{(v, w, x) \,|v = \zeta_r(w), w \geq w_\ell\}.$$

In Ω_ℓ, the dynamics is governed by the following system.

$$\begin{aligned} \frac{dw}{dt} &= h(\zeta_\ell(w), w) + \delta p(w, x), \\ \frac{dx}{dt} &= -\epsilon\delta p(w, x). \end{aligned} \tag{11}$$

This system is valid in the region Λ_ℓ defined by

$$\Lambda_\ell = \{(w, x) \,|\geq w_\ell\}.$$

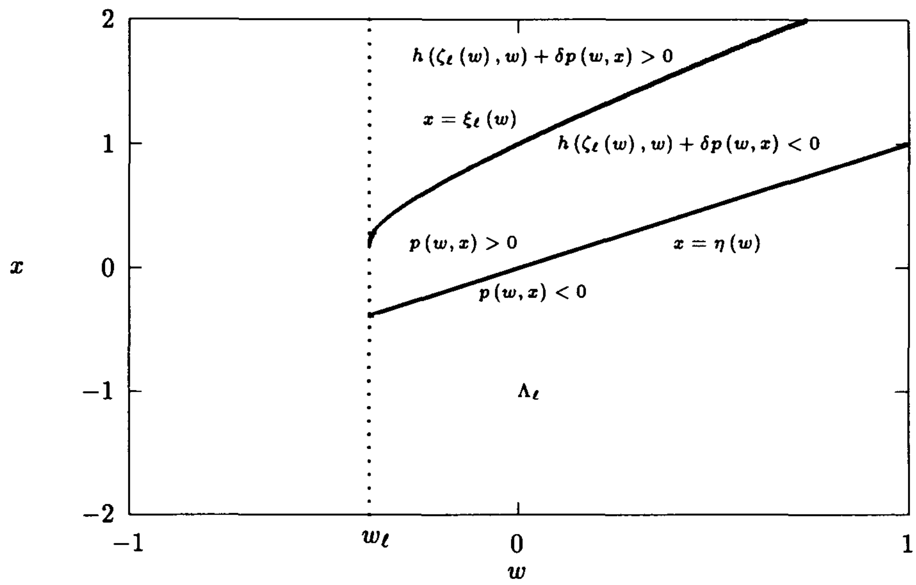

Figure 7: The region Λ_ℓ. The nullclines of (11) which is obtained from (8) are shown.

Similarly, in Ω_r, the dynamics is governed by the system

$$\begin{aligned} \frac{dw}{dt} &= h(\zeta_r(w), w) + \delta p(w, x), \\ \frac{dx}{dt} &= -\epsilon\delta p(w, x), \end{aligned} \tag{12}$$

which is valid in the region Λ_r difined by

$$\Lambda_r = \{(w, x) \,|\geq w_r\}.$$

Figures (7) and (8) show some examples of nullclines of (11) and (12), respectively. Figures 9 and 10 show some examples of trajectories of solutions of (11) and (12), respectively.

In the limit $\kappa \longrightarrow 0$, we define solutions of (4) using solutions of (11) and (12). We denote by $\phi(t, P_0)$ the solution of (4) with the initial value $\phi(0, P_0) = P_0$. We also denote by $\phi_\ell(t, Q_0) = (\gamma_\ell(t, Q_0), \sigma_\ell(t, Q_0))$ the solution of (11) with the initial value $\phi_\ell(0, Q_0) = Q_0$, and by $\tau_\ell(Q_0)$ the time it takes for $\phi_\ell(t, Q_0)$ to reach the lines $w = w_\ell$. Similarly, we denote by $\phi_r(t, Q_0) = (\gamma_r(t, Q_0), \sigma_r(t, Q_0))$ the solution of (12) with the initial value $\phi_r(0, Q_0) = Q_0$, and by $\tau_r(Q_0)$ the time it takes for $\phi_r(t, Q_0)$ to reach the lines $w = w_r$. Suppose that $P_0 = (v_0, w_0, x_0) = (\zeta_\ell(w_0), w_0, x_0) \in \Omega_\ell$ with $Q_0 = (w_0, x_0) \in \Lambda_\ell$, Then

$$\phi(t, P_0) = (\zeta_\ell(\gamma_\ell(t, Q_0)), \gamma_\ell(t, Q_0), \sigma_\ell(t, Q_0))$$

for $0 \leq t < \tau_\ell(Q_0)$. Suppose that $Q_1 = (w_\ell, x_1) = \phi_\ell(\tau_\ell(Q_0), Q_0)$. At $t = \tau_\ell(Q_0)$, $\phi(t, P_0)$ jumps to the point $(\zeta_r(w_\ell), w_\ell, x_1)$, and for $\tau_\ell(Q_0) \leq t < \tau_\ell(Q_0) + \tau_r(Q_1)$,

$$\phi(t, P_0) = (\zeta_r(\gamma_r(t - \tau_\ell(Q_0), Q_1)), \gamma_r(t - \tau_\ell(Q_0), Q_1), \sigma_r(t - \tau_\ell(Q_0), Q_1)).$$

Suppose that $Q_2 = (w_r, x_2) = \phi_r(\tau_r(Q_1), Q_1)$. At $t = \tau_\ell(Q_0) + \tau_r(Q_1)$, $\phi(t, P_0)$ jumps to the point $(\zeta_\ell(w_r), w_r, x_2)$. In particular, $\phi(t, P_0)$ is a periodic solution provided that $w_0 = w_r$ and that $x_0 = x_2$. Now we define the map Φ by $\Phi(x_0) = x_2$, where

$$\begin{aligned} Q_0 &= (w_r, x_0), \\ Q_1 &= (w_\ell, x_1) = \phi_\ell(\tau_\ell(Q_0), Q_0), \\ Q_2 &= (w_r, x_2) = \phi_r(\tau_r(Q_1), Q_1) \end{aligned}$$

(Cf. figure 11). It follows that a fixed point of Φ corresponds to a periodic solution of (4). Such a periodic

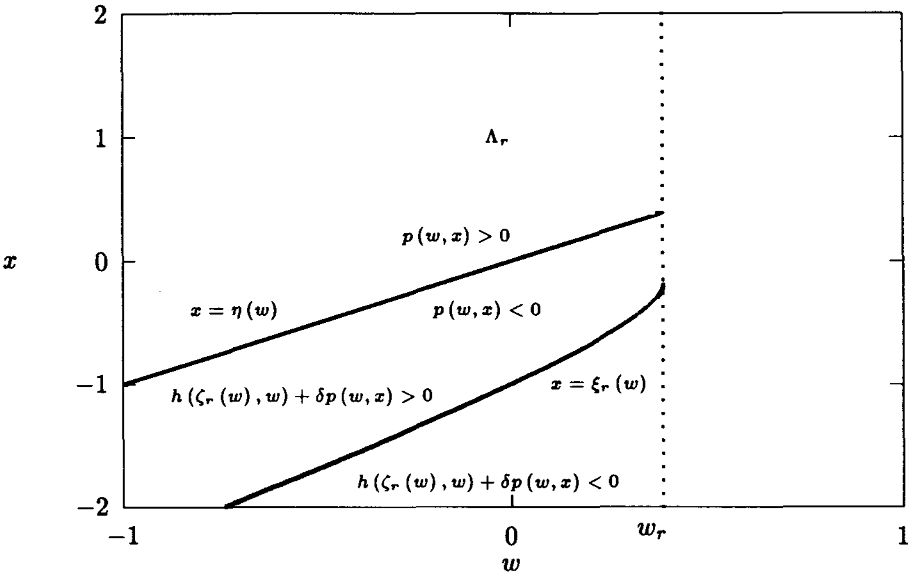

Figure 8: The region Λ_r. The nullclines of (12) which is obtained from (8) are shown.

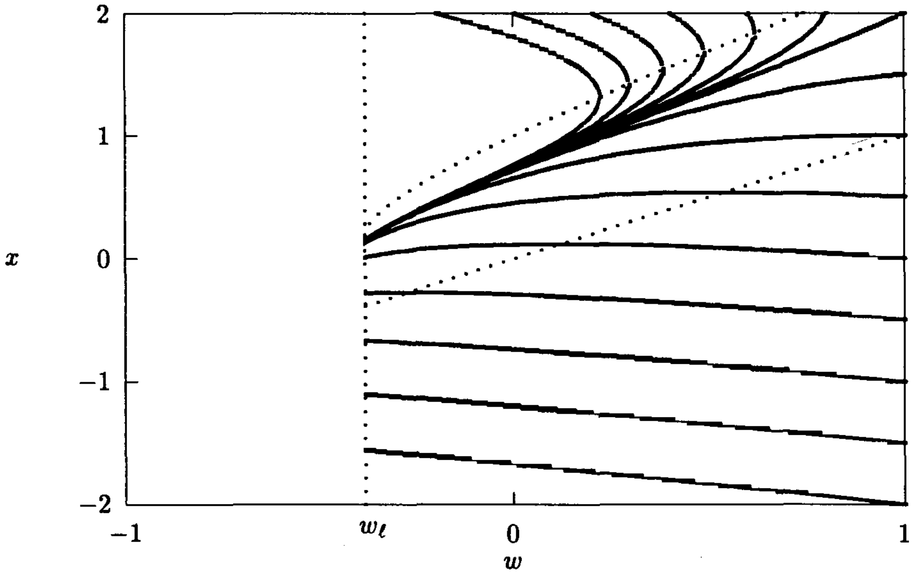

Figure 9: Trajectories in Λ_ℓ. Some trajectories of solutions of (11) which is obtained from (8) are shown.

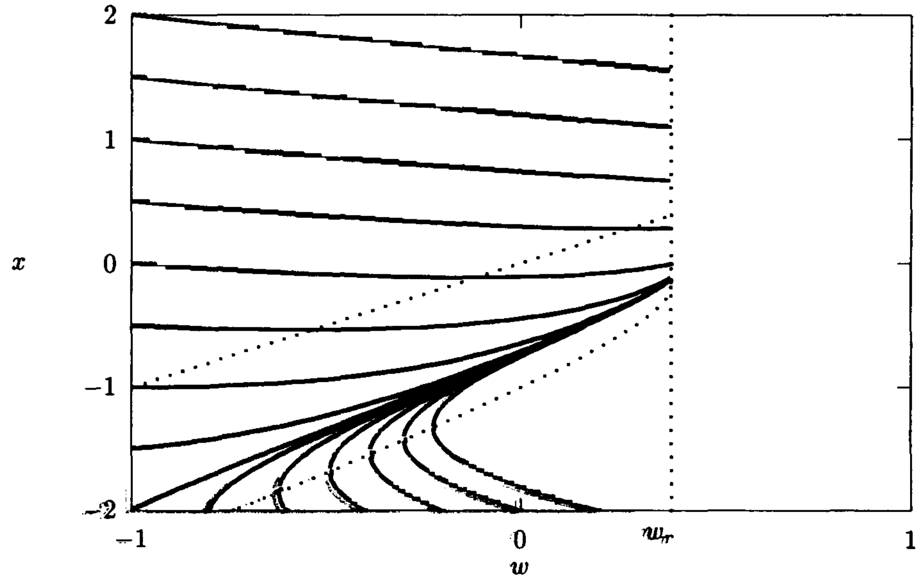

Figure 10: Trajectories in Λ_r. Some trajectories of solutions of (12) which is obtained from (8) are shown.

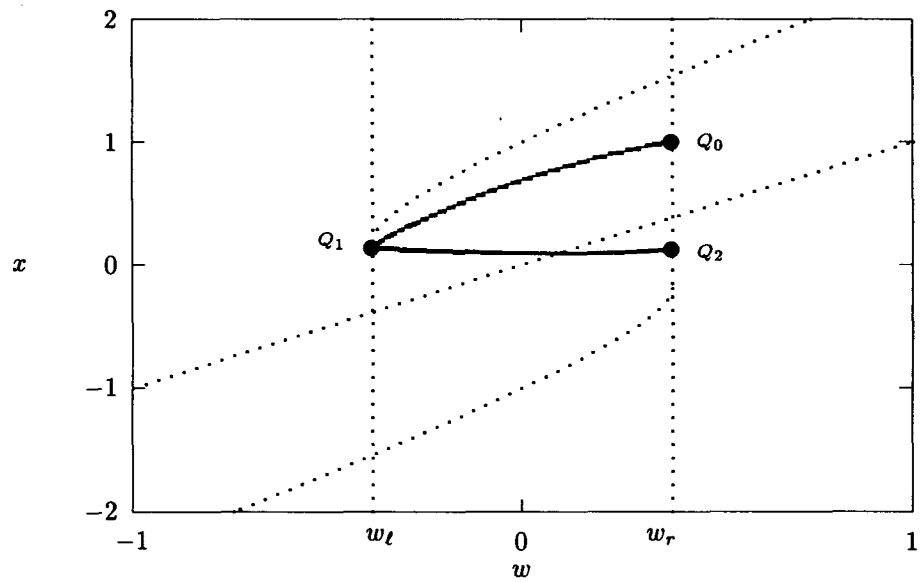

Figure 11: The definition of the map Φ. The map Φ is defined by $\Phi(x_0) = x_2$, where $Q_0 = (w_r, x_0)$, $Q_1 = (w_\ell, x_1) = \phi_\ell(\tau_\ell(Q_0), Q_0)$, $Q_2 = (w_r, x_2) = \phi_r(\tau_r(Q_1), Q_1)$. Here (11) and (12) are obtained from (8), and the map is numerically generated.

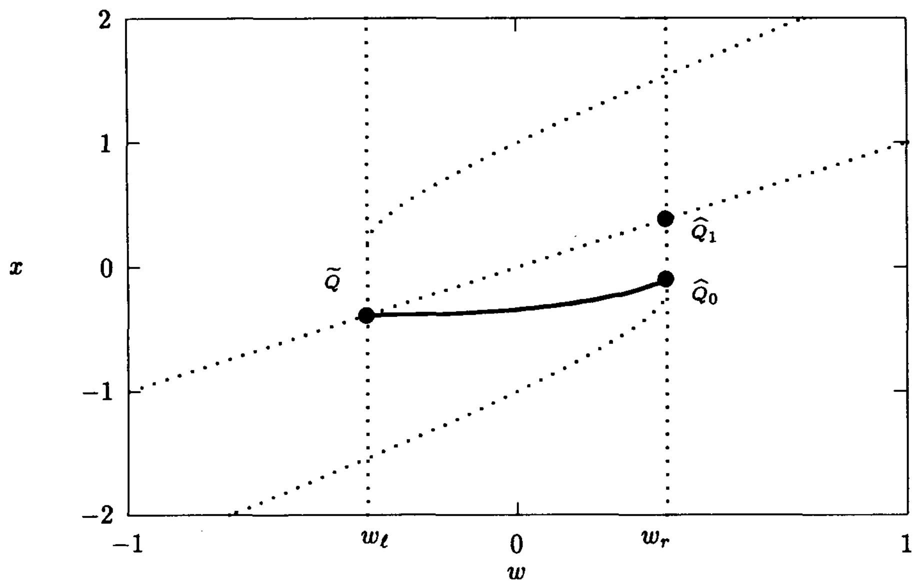

Figure 12: The invariant interval of the map. $\widetilde{Q}$, $\widehat{Q}_0$, and $\widehat{Q}_1$ are defined by $\widetilde{Q} = (w_\ell, \eta(w_\ell))$, $\widehat{Q}_0 = (w_r, \widehat{x}_0) = \phi_r\left(\tau_r\left(\widetilde{Q}\right), \widetilde{Q}\right)$, and $\widehat{Q}_1 = (w_r, \widehat{x}_1) = (w_r, \eta(w_r))$. Then $[\widehat{x}_0, \widehat{x}_1]$ is an invariant interval of the map Φ. Here (11) and (12) are obtained from (8).

solution is discontinuous. When a discontinuous periodic solution in the singular limit exists, (4) can have at least one periodic solution for all sufficiently small $\kappa > 0$. Orbits of such periodic solutions are close to the orbit of the discontinuous periodic solution [1].

3. Periodic Solutions in the Singular Limit

In this section, we show that the map constructed in Section 2 always has a fixed point for a given pair (δ, ϵ). Let $\widetilde{Q} = (w_\ell, \eta(w_\ell))$, let $\widehat{Q}_0 = (w_r, \widehat{x}_0) = \phi_r\left(\tau_r\left(\widetilde{Q}\right), \widetilde{Q}\right)$, and let $\widehat{Q}_1 = (w_r, \widehat{x}_1) = (w_r, \eta(w_r))$ (cf. Figure 12). It is easily seen that the interval $[\widehat{x}_0, \widehat{x}_1]$ is an invariant interval of Φ. It follows that Φ has a fixed point in the interval $[\widehat{x}_0, \widehat{x}_1]$ for Φ is continuous. Moreover, using a method in [6], it can be shown that

$$0 < \Phi'(x_0) < 1$$

for $x_0 \in [\widehat{x}_0, \widehat{x}_1]$. Therefore Φ has a unique fixed point in the interval $[\widehat{x}_0, \widehat{x}_1]$.

Some examples of periodic solutions of (8) are shown in Figures 13 and 14. Suppose that

$$\xi_\ell(w_\ell) = \xi_r(w_r)$$

for $\delta = \delta^*$. As $\epsilon \longrightarrow 0$, some numerical results indicates that the period approaches some finite value for $0 < \delta < \delta^*$, and that the period diverges to infinity for $\delta > \delta^*$ For some values of ϵ between 0.01 and 0.5, The fixed points of the map Φ are numerically generated and shown in Figures 15 and 17, and The period of the periodic solutions are numerically computed and shown in Figures 16 and 18. For Figures 15 and 16, $\delta = 1$ for which $\xi_\ell(w_\ell) > \xi_r(w_r)$. For Figures 17 and 18, $\delta = 2$ for which $\xi_\ell(w_\ell) < \xi_r(w_r)$.

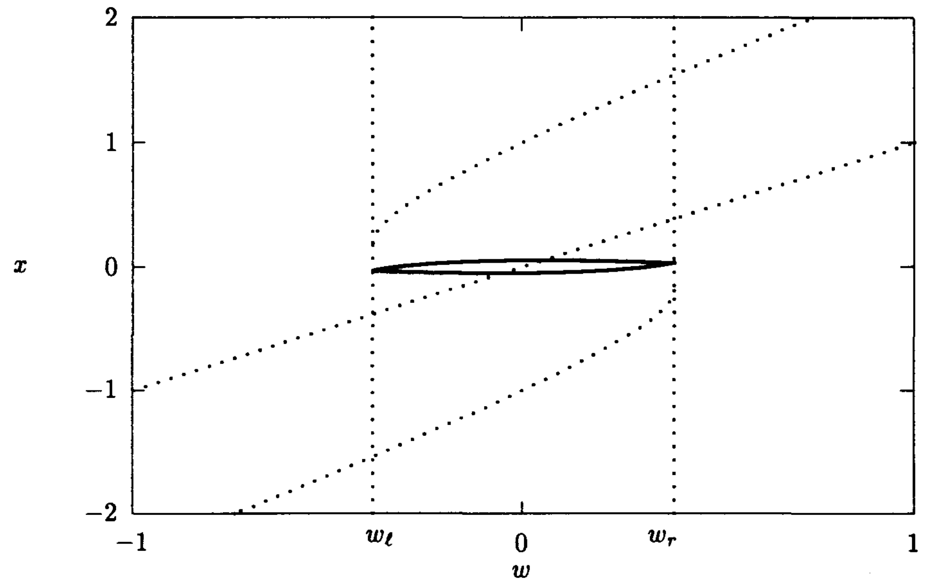

Figure 13: A periodic solution of the singular system. A periodic solution of (8) in the limit $\kappa \longrightarrow 0$ is numerically generated. Here $\delta = 1$ and $\epsilon = 0.5$. The period T of the periodic solution is given approximately by $T \approx 1.974587$.

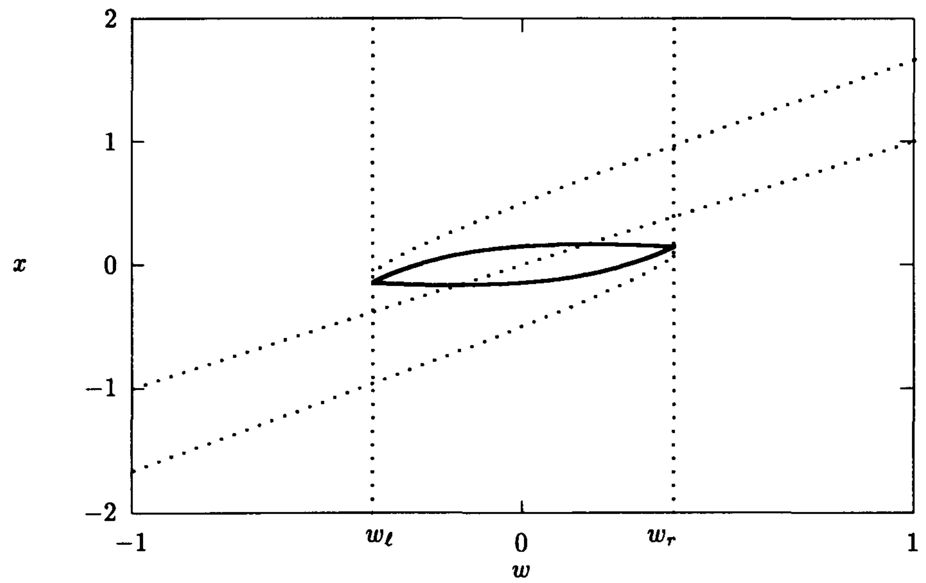

Figure 14: A periodic solution of the singular system. A periodic solution of (8) in the limit $\kappa \longrightarrow 0$ is numerically generated. Here $\delta = 2$ and $\epsilon = 0.5$. The period T of the periodic solution is given approximately by $T \approx 3.084079$.

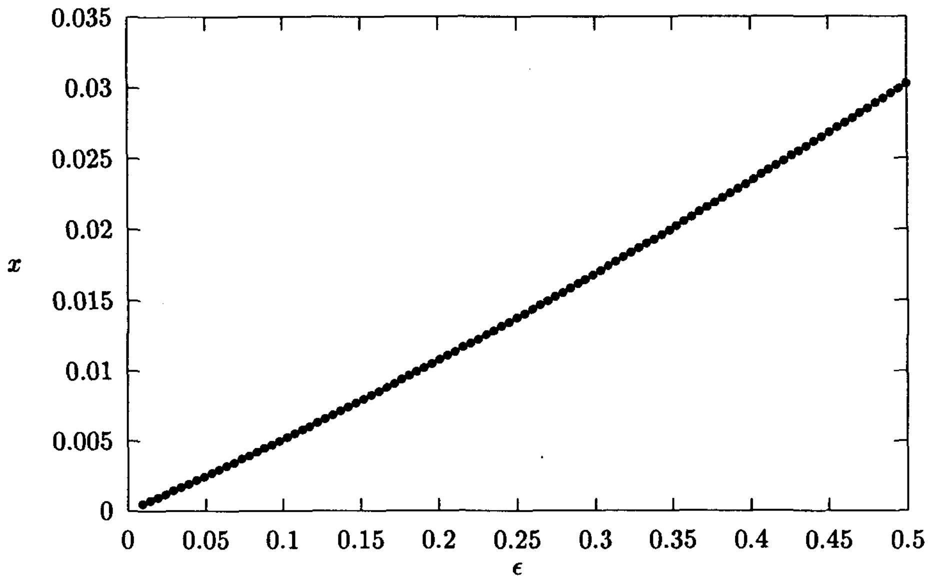

Figure 15: The fixed points of the map. Here (11) and (12) are obtained from (8), and the fixed points of the map Φ are numerically generated for $\delta = 1$ and for some values of ϵ between 0.01 and 0.5.

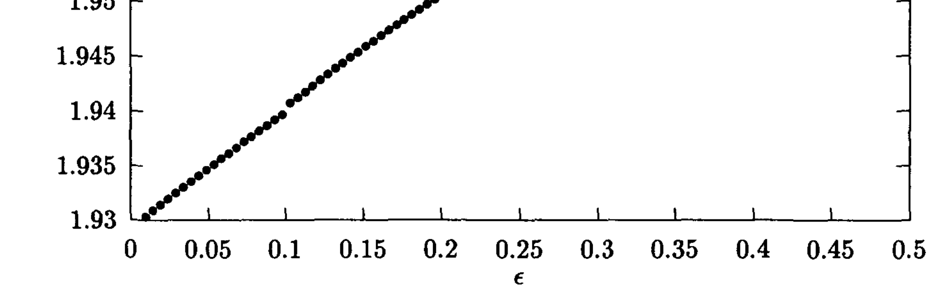

Figure 16: The period of the periodic solutions in the singular limit. The period of the periodic solutions of (8) in the singular limit is numerically generated for $\delta = 1$ and for some values of ϵ between 0.01 and 0.5.

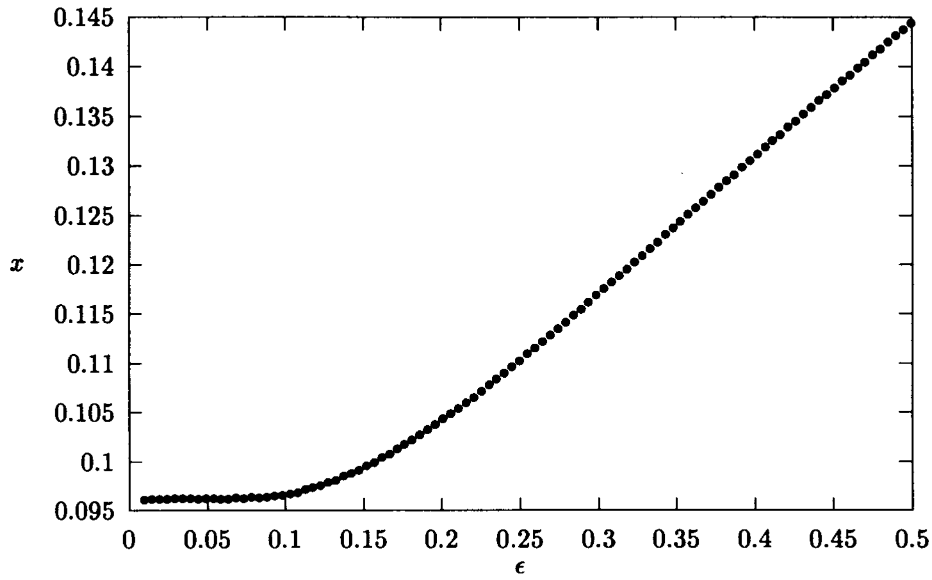

Figure 17: The fixed points of the map. Here (11) and (12) are obtained from (8), and the fixed points of the map Φ are numerically generated for $\delta = 2$ and for some values of ϵ between 0.01 and 0.5.

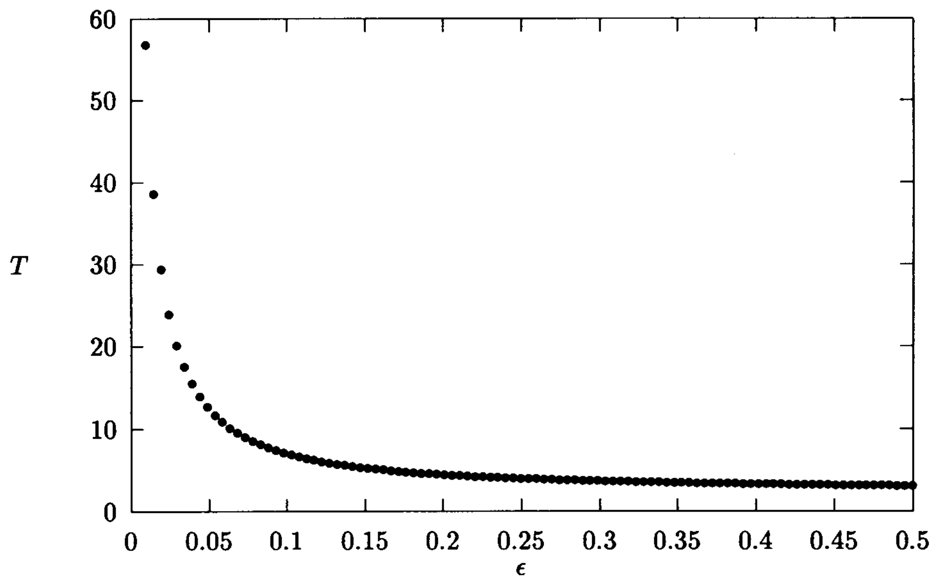

Figure 18: The period of the periodic solutions in the singular limit. The period of the periodic solutions of (8) in the singular limit is numerically generated for $\delta = 2$ and for some values of ϵ between 0.01 and 0.5.

REFERENCES

[1] E. F. Mishchenko and N. Kh. Rozov, Differential Equations with Small Parameters and Relaxation Oscillations, Translated from Russian by F. M. C. Goodspeed (Diffrentsial'nye Uravneniia s malym parametrom i reksatsinnye kolenbaniia), Plenum Press, New York, 1980.

[2] Hans G. Othmer and John A. Aldridge, The effects of cell density and metabolite flux on cellular dynamics, J. Math. Biology **5** (1978), 169-200.

[3] Morris W. Hirsch and Stephen Smale, Differential Equations, Dynamical Systems, and Linear Algebra, Academic Press, New York, 1974.

[4] Masaji Watanabe, Bifurcation of synchronized periodic solutions in systems of coupled oscillators, I: Perturbation results for weak and strong coupling, Rocky Mountain Journal of Mathematics **23** (4) (1993), 1483-1525.

[5] Masaji Watanabe, Bifurcation of synchronized periodic solutions in systems of coupled oscillators, II: Global bifurcation in coupled planar oscillators, Rocky Mountain Journal of Mathematics **23** (4) (1993), 1527-1554.

[6] Masaji Watanabe, On long-period oscillations in coupled systems of nonlinear oscillators and stationary systems, Journal of the Faculty of the Environmental Science and Technology, Okayama University, **2** (1) (1997), 19-24.